arXiv:2312.16476v6 [cs.CV] 17 Dec 2024

SVGDreamer: Text Guided SVG Generation with Diffusion Model

Ximing Xing, Haitao Zhou, Chuang Wang, Jing Zhang
Beihang University
{ximingxing, zhouhaitao, chuangwang, zhang_jing}@buaa.edu.cn

Dong Xu
The University of Hong Kong
dongxu@cs.hku.hk

Qian Yu*
Beihang University
qianyu@buaa.edu.cn

Abstract

Recently, text-guided scalable vector graphics (SVGs) synthesis has shown promise in domains such as iconography and sketch. However, existing text-to-SVG generation methods lack editability and struggle with visual quality and result diversity. To address these limitations, we propose a novel text-guided vector graphics synthesis method called SVGDreamer. SVGDreamer incorporates a semantic-driven image vectorization (SIVE) process that enables the decomposition of synthesis into foreground objects and background, thereby enhancing editability. Specifically, the SIVE process introduces attention-based primitive control and an attention-mask loss function for effective control and manipulation of individual elements. Additionally, we propose a Vectorized Particle-based Score Distillation (VPSD) approach to address issues of shape over-smoothing, color over-saturation, limited diversity, and slow convergence of the existing text-to-SVG generation methods by modeling SVGs as distributions of control points and colors. Furthermore, VPSD leverages a reward model to re-weight vector particles, which improves aesthetic appeal and accelerates convergence. Extensive experiments are conducted to validate the effectiveness of SVGDreamer, demonstrating its superiority over baseline methods in terms of editability, visual quality, and diversity. Project page: https://ximinng.github.io/SVGDreamer-project/

1. Introduction

Scalable Vector Graphics (SVGs) represent visual concepts using geometric primitives such as Bézier curves, polygons, and lines. Due to their inherent nature, SVGs are highly suitable for visual design applications, such as posters and logos. Secondly, compared to raster images, vector images can maintain compact file sizes, making them more efficient for storage and transmission purposes. More importantly, vector images offer greater editability, allowing designers to easily select, modify, and compose elements. This attribute is particularly crucial in the design process, as it allows for seamless adjustments and creative exploration.

In recent years, there has been a growing interest in general vector graphics generation. Various optimization-based methods [4, 12, 19, 28, 34, 40, 41, 48] have been proposed, building upon the differentiable rasterizer DiffVG [14]. These methods, such as CLIPDraw [4] and VectorFusion [12], differ primarily in their approach to supervision. Some works [4, 19, 28, 34, 40, 41] combine the CLIP model [23] with DiffVG [14], using CLIP as a source of supervision. More recently, the significantly progress achieved by Text-to-Image (T2I) diffusion models [20, 24, 26, 27, 37] has inspired the task of text-to-vector-graphics. Both VectorFusion [12] and DiffSketcher [48] attempted to utilize T2I diffusion models for supervision. These models make use of the high-quality raster images generated by T2I models as targets to optimize the parameters of vector images. Additionally, the priors embedded within T2I models can be distilled and applied in this task. Consequently, models that use T2I for supervision generally perform better than those using the CLIP model.

Despite their impressive performance, existing T2I-based methods have certain limitations. Firstly, the vector images generated by these methods lack editability. Unlike the conventional approach of creating vector graphics, where individual elements are added one by one, T2I-based methods do not distinguish between different components during synthesis. As a result, the objects become entangled, making it challenging to edit or modify a single object independently. Secondly, there is still a large room for improvement in visual quality and diversity of the re-

*Corresponding author

sults generated by these methods. Both VectorFusion [12] and DiffSketcher [48] extended the Score Distillation Sampling (SDS) [22] to distill priors from the T2I models. However, it has been observed that SDS can lead to issues such as color over-saturation and over-smoothing, resulting in a lack of fine details in the generated vector images. Besides, SDS optimizes a set of control points in the vector graphic space to obtain the average state of the vector graphic corresponding to the text prompt in a mode-seeking manner [22]. This leads to a lack of diversity and detailed construction in the SDS-based approach [12, 48], along with absent text prompt objects.

To address the aforementioned issues, we present a new model called SVGDreamer for text-guided vector graphics generation. Our primary objective is to produce vector graphics of superior quality that offer enhanced editability, visual appeal, and diversity. To ensure editability, we propose a semantic-driven image vectorization (SIVE) process. This approach incorporates an innovative attention-based primitive control strategy, which facilitates the decomposition of the synthesis process into foreground objects and background. To initialize the control points for each foreground object and background, we leverage cross-attention maps queried by text tokens. Furthermore, we introduce an attention-mask loss function, which optimizes the graphic elements hierarchically. The proposed SIVE process ensures the separation and editability of the individual elements, promoting effective control and manipulation of the resulting vector graphics.

To improve the visual quality and diversity of the generated vector graphics, we introduce Vectorized Particle-based Score Distillation (VPSD) for vector graphics refinement. Previous works in vector graphics synthesis [11, 12, 48] that utilized SDS often encountered issues like shape over-smoothing, color over-saturation, limited diversity, and slow convergence in synthesized results [22, 48]. To address these issues, VPSD models SVGs as distributions of control points and colors, respectively. VPSD adopts a LoRA [10] network to estimate these distributions, aligning vector graphics with the pretrained diffusion model. Furthermore, to enhance the aesthetic appeal of the generated vector graphics, we integrate ReFL [49] to fine-tune the estimation network. Through this refinement process, we achieve final vector graphics that exhibit high editability, superior visual quality, and increased diversity. To validate the effectiveness of our proposed method, we perform extensive experiments to evaluate the model across multiple aspects. In summary, our contributions can be summarized as follows:

- We introduce *SVGDreamer*, a novel model for text-to-SVG generation. This novel model is capable of generating high-quality vector graphics while preserving editability.
- We present the semantic-driven image vectorization (SIVE) method, which ensures that the generated vector objects are separate and flexible to edit. Additionally, we propose the vectorized particle-based score distillation (VPSD) loss to guarantee that the generated vector graphics exhibit both exceptional visual quality and a wide range of diversity.
- We conduct comprehensive experiments to evaluate the effectiveness of our proposed method. Results demonstrate the superiority of our approach compared to baseline methods. Moreover, our model showcases strong generalization capabilities in generating diverse types of vector graphics.

2. Related Work

2.1. Vector Graphics Generation

Scalable Vector Graphics (SVGs) offer a declarative format for visual concepts expressed as primitives. One approach to creating SVG content is to use Sequence-To-Sequence (seq2seq) models to generate SVGs [1, 5, 16, 25, 43, 44, 46]. These methods heavily rely on dataset in vector form, which limits their generalization ability and their capacity to synthesize complex vector graphics. Instead of directly learning an SVG generation network, an alternative method of vector synthesis is to optimize towards a matching image during evaluation time.

Li *et al.* [14] introduce a differentiable rasterizer that bridges the vector graphics and raster image domains. While image generation methods that traditionally operate over vector graphics require a vector-based dataset, recent work has demonstrated the use of differentiable renderers to overcome this limitation [17, 25, 28, 30, 36, 38, 39, 48]. Furthermore, recent advances in visual text embedding contrastive language-image pre-training model (CLIP) [23] have enabled a number of successful methods for synthesizing sketches, such as CLIPDraw[4], CLIP-CLOP [19], and CLIPasso [40]. A very recent work VectorFusion [12] and DiffSketcher [48] combine differentiable renderer with text-to-image diffusion model for vector graphics generation, resulting in promising results in fields such as iconography, pixel art, and sketch.

2.2. Text-to-Image Diffusion Model

Denoising diffusion probabilistic models (DDPMs) [8, 31, 33, 35], particularly those conditioned on text, have shown promising results in text-to-image synthesis. For example, Classifier-Free Guidance (CFG) [7] has improved visual quality and is widely used in large-scale text conditional diffusion model frameworks, including GLIDE [20], Stable Diffusion [26], DALL·E 2 [24], Imagen [27] and DeepFloyd IF [37]. The progress achieved by text-to-image diffusion models [20, 24, 26, 27] also promotes the devel-

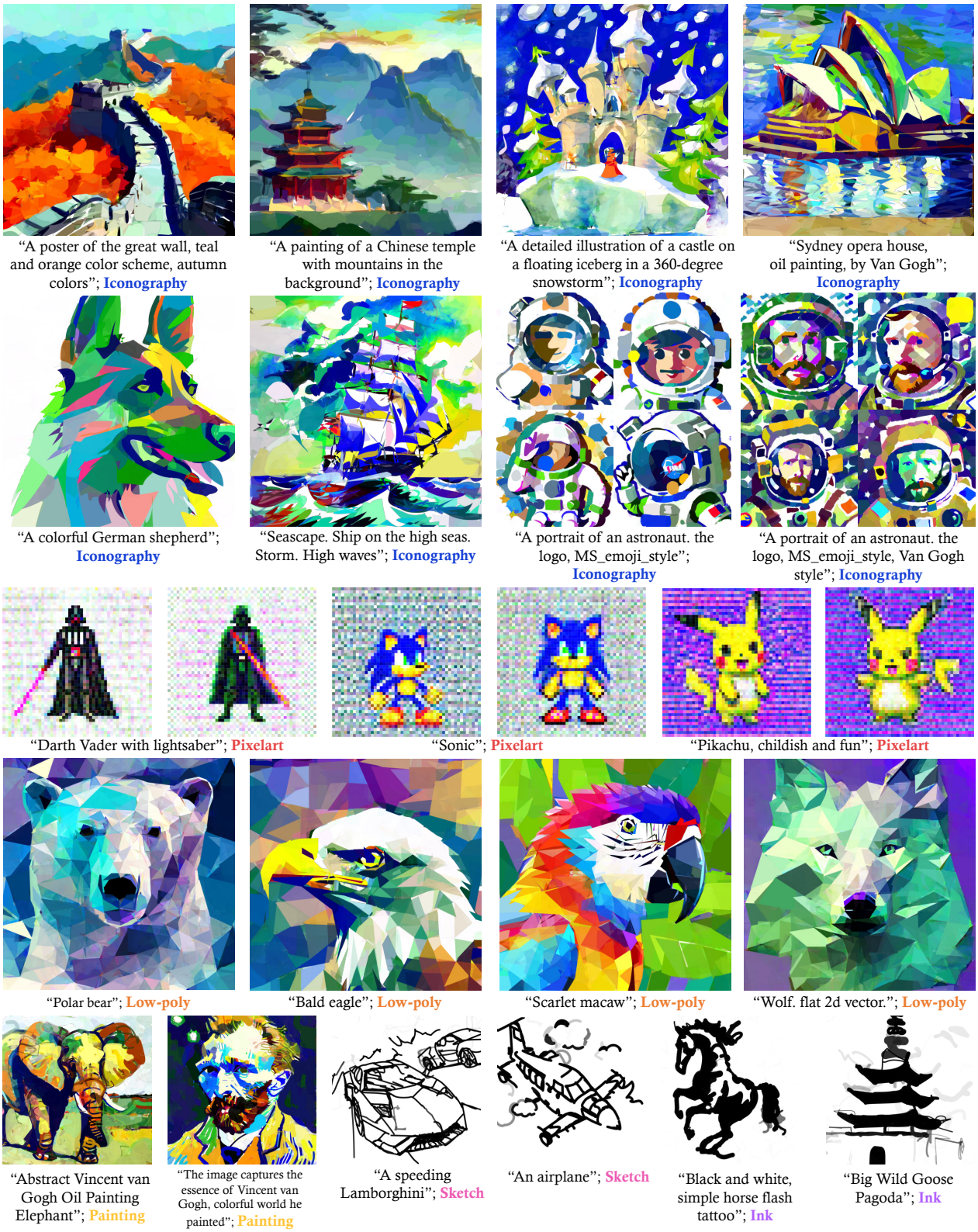


Figure 1. Given a text prompt, SVGDreamer can generate a variety of vector graphics. SVGDreamer is a versatile tool that can work with various vector styles without being limited to a specific prompt suffix. We utilize various colored suffixes to indicate different styles. The style is governed by vector primitives.

opment of a series of text-guided tasks, such as text-to-3D [22]. In this work, we employ Stable Diffusion model to provide supervision for text-to-SVG generation.

2.3. Score Distillation Sampling

Recent advances in natural image modeling have sparked significant research interest in utilizing powerful 2D pre-trained models to recover 3D object structures [15, 18, 21, 22, 42, 45]. Recent efforts such as DreamFusion [22], Magic3D [15] and Score Jacobian Chaining [42] explore text-to-3D generation by exploiting a score distillation sampling (SDS) loss derived from a 2D text-to-image diffusion model [26, 27] instead, showing impressive results. The development of text-to-SVG [12, 48] was inspired by this, but the resulting vector graphics have limited quality and exhibit a similar over-smoothness as the reconstructed 3D models. Wang *et al.* [45] extend the modeling of the 3D model as a random variable instead of a constant as in SDS and present variational score distillation to address the over-smoothing issues in text-to-3D generation.

3. Methodology

In this section, we introduce SVGDreamer, an optimization-based method that creates a variety of vector graphics based on text prompts. We define a vector graphic as a set of paths $\{P_i\}_{i=1}^n$ and color attributes $\{C_i\}_{i=1}^n$. Each path consists of m control points $P_i = \{p_j\}_{j=1}^m = \{(x_j, y_j)\}_{j=1}^m$ and one color attribute $C_i = \{r, g, b, a\}_i$. We optimize an SVG by back-propagating gradients of rasterized images to SVG path parameters $\theta = \{P_i, C_i\}_{i=1}^n$ via a differentiable renderer $\mathcal{R}(\theta)$ [14].

Our approach leverages the text-to-image diffusion model prior to guide the differentiable renderer $\mathcal{R}$ and optimize the parametric graphic path θ, resulting in the synthesis of vector graphs that match the description of the text prompt y. As illustrated in Fig. 2, our pipeline consists of two parts: semantic-driven image vectorization and SVG synthesis through VPSD optimization. The first part is **S**emantic-driven **I**mage **VE**ctorization (SIVE), consisting of two stages: primitive initialization and semantic-aware optimization. We rethink the application of attention mechanisms in synthesizing vector graphics. We extract the cross-attention maps corresponding to different objects in the diffusion model and apply it to initialize control points and consolidate object vectorization. This process allows us to decompose the foreground objects from the background. Consequently, the SIVE process generates vector objects which are independently editable. It separates vector objects by aggregating the curves that form them, which in turn simplifies the combination of vector graphics.

In Sec. 3.2, we propose the **V**ectorized **P**article-based **S**core **D**istillation (VPSD) to generate diverse high-quality text-matching vector graphics. VPSD is designed to model the distribution of vector path control points and colors for approximating the vector parameter distribution, thus obtaining vector results of diversity.

3.1. SIVE: Semantic-driven Image Vectorization

Image rasterization is a mature technique in computer graphics, while image vectorization, the reverse path of rasterization, remains a major challenge. Given an arbitrary input image, LIVE [17] recursively learns the visual concepts by adding new optimizable closed Bézier paths and optimizing all these paths. However, LIVE [17] struggles with grasping and distinguishing various subjects within an image, leading to identical paths being superimposed onto different visual subjects. And the LIVE-based method [12, 17] fails to represent intricate vector graphics consisting of complex paths. We propose a semantic-driven image vectorization method to address the aforementioned issue. This method consists of two main stages: primitive initialization and semantic-aware optimization. In the initialization stage, we allocate distinct control points to different regions corresponding to various visual objects with the guidance of attention maps. In the optimization stage, we introduce an attention-based mask loss function to hierarchically optimize the vector objects.

3.1.1 Primitive Initialization

Vectorizing visual objects often involves assigning numerous paths, which leads to *object-layer confusion* in LIVE-based methods. To address this issue, we suggest organizing vector graphic elements semantically and assigning paths to objects based on their semantics. We initialize O groups of object-level control points according to the cross-attention map corresponding to different objects in the text prompt. And we represent them as the foreground $\mathcal{M}_{\text{FG}}^i$, where i indicates the i-th token in the text prompt. Correspondingly, the rest will be treated as background. Such design allows us to represent the attention maps of background and foreground as,

$$\begin{aligned} \mathcal{M}_{\text{BG}} &= 1 - (\sum_{i=1}^{O} \mathcal{M}_{\text{FG}}^i); \\ \mathcal{M}_{\text{FG}}^i &= \text{softmax}(QK_i^T)/\sqrt{d} \end{aligned} \tag{1}$$

where $\mathcal{M}_{\text{BG}}$ indicates the attention map of the background. $\mathcal{M}_{\text{FG}}^i$ indicates cross-attention score, where K_i indicates i-th token keys from text prompt, Q is pixel queries features, and d is the latent projection dimension of the keys and queries.

Then, inspired by DiffSketcher [48], we normalize the attention maps using softmax and treat it as a distribution map to sample m positions for the first control point $p_{j=1}$ of each Bézier curve. The other control points ($\{p_j\}_{j=2}^m$) are sampled within a small radius (0.05 of image size) around $p_{j=1}$ to define the initial set of paths.

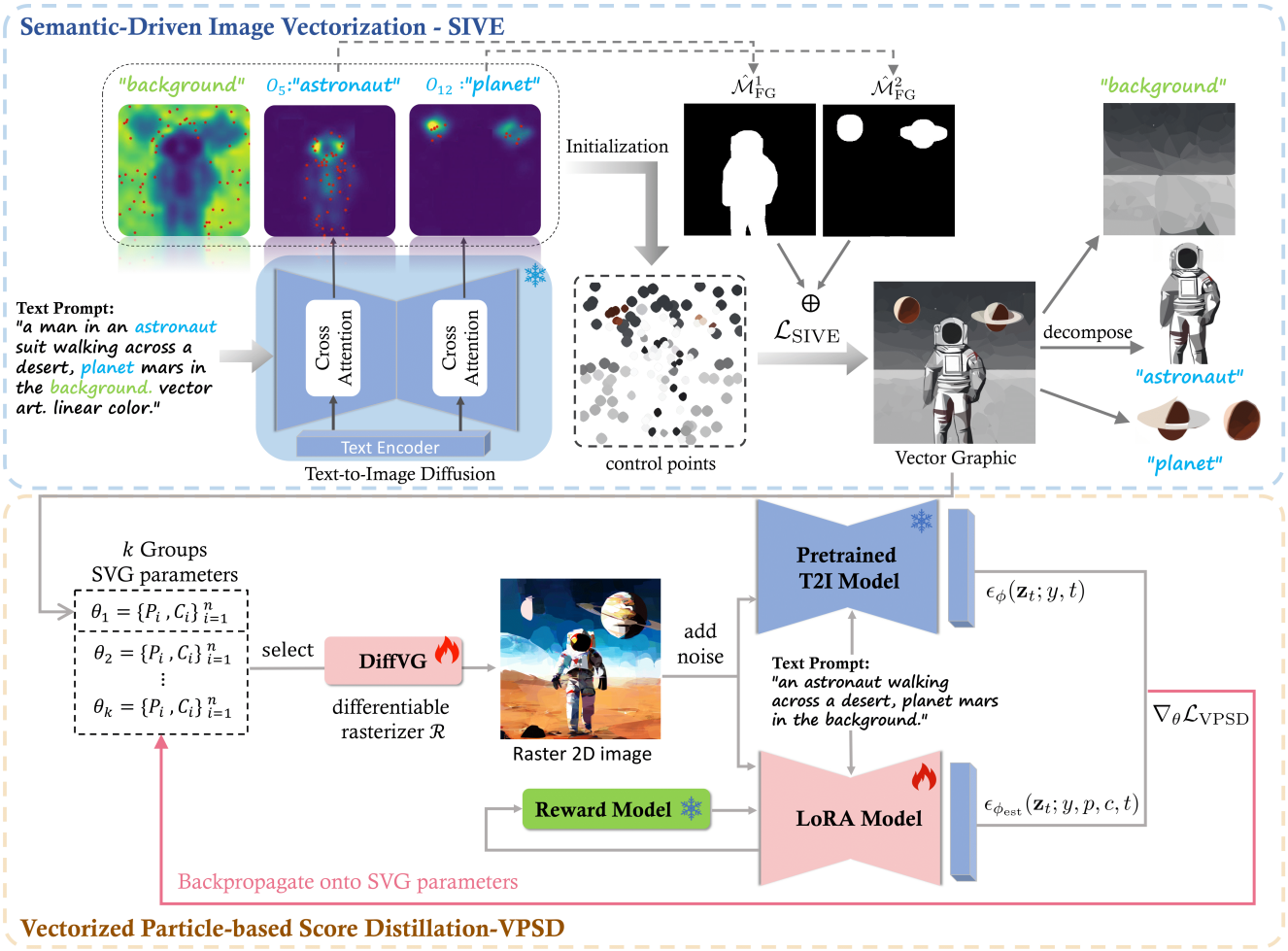


Figure 2. **Overview of SVGDreamer.** The method consists of two parts: semantic-driven image vectorization (SIVE, Sec. 3.1) and SVG synthesis through VPSD optimization (Sec. 3.2). The result obtained from SIVE can be used as input of VPSD for further refinement.

3.1.2 Semantic-aware Optimization

In this stage, we utilize an attention-based mask loss to separately optimize the objects in the foreground and background. This ensures that control points remain within their respective regions, aiding in object decomposition. Namely, the hierarchy only exists within the designated object and does not get mixed up with other objects. This strategy fuels the permutations and combinations between objects that form different vector graphics, and enhances the editability of the objects themselves.

Specifically, we convert the attention map obtained during the initialization stage into reusable masks $\hat{\mathcal{M}} = \{\{\hat{\mathcal{M}}_{\text{FG}}\}_{o=1}^{O}, \hat{\mathcal{M}}_{\text{BG}}\}$, O foregrounds and one background mask in total. We do this by setting the attention score to 1 if it is greater than the threshold value, and to 0 otherwise.

$$\mathcal{L}_{\text{SIVE}} = \sum_{i}^{O} \left(\hat{\mathcal{M}}_i \odot I - \hat{\mathcal{M}}_i \odot \mathbf{x} \right)^2 \tag{2}$$

where I is the target image, $\hat{\mathcal{M}}$ is mask, $\mathbf{x} = \mathcal{R}(\theta)$ is the rendering.

3.2. Vectorized Particle-based Score Distillation

While vectorizing a rasterized diffusion sample is lossy, recent techniques [12, 48] have identified the SDS loss [22] as beneficial for our task of generating vector graphics. To synthesize a vector image that matches a given text prompt y, they directly optimize the parameters $\theta = \{P_i, C_i\}_{i=1}^n$ of a differentiable rasterizer $\mathcal{R}(\theta)$ via SDS loss. At each iteration, the differentiable rasterizer is used to render a raster image $\mathbf{x} = \mathcal{R}(\theta)$, which is augmented to obtain a $\mathbf{x}_a$. Then, the pretrained latent diffusion model (LDM) ϵ_ϕ uses a VAE encoder [3] to encode $\mathbf{x}_a$ into a latent representation $\mathbf{z} = \mathcal{E}(\mathbf{x_a})$, where $\mathbf{z} \in \mathbb{R}^{(H/f)\times(W/f)\times 4}$ and f is the encoder downsample factor. Finally, the gradient of SDS is

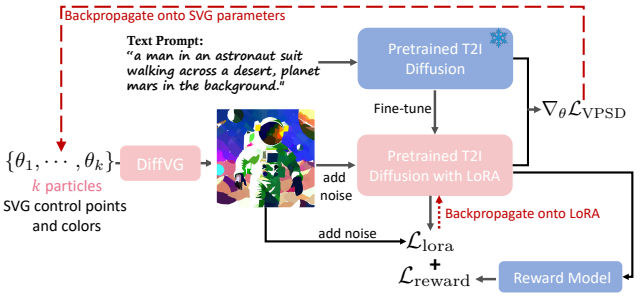


Figure 3. **The process of Vectorized Particle-based Score Distillation.** VPSD allows k SVGs as input and simultaneously optimizes k sets of SVG parameters.

estimated by,

$$\nabla_\theta \mathcal{L}_{\text{SDS}}(\phi, \mathbf{x} = \mathcal{R}(\theta)) \triangleq \mathbb{E}_{t,\epsilon,a}\left[w(t)(\epsilon_\phi(\mathbf{z}_t; y, t) - \epsilon) \frac{\partial \mathbf{z}}{\partial \mathbf{x}_a} \frac{\partial \mathbf{x}_a}{\partial \theta} \right] \tag{3}$$

where $w(t)$ is the weighting function. And noised to form $\mathbf{z}_t = \alpha_t \mathbf{x}_a + \sigma_t \epsilon$.

Unfortunately, SDS-based methods often suffer from issues such as shape over-smoothing, color over-saturation, limited diversity in results, and slow convergence in synthesis results [11, 12, 22, 48]. Inspired by the principled variational score distillation framework [45], we propose vectorized particle-based score distillation (VPSD) to address the aforementioned issues. Instead of modeling SVGs as a set of control points and corresponding colors like SDS, we model SVGs as the distributions of control points and colors respectively. In principle, given a text prompt y, there exists a probabilistic distribution μ of all possible vector shapes representations. Under a vector representation parameterized by θ, such a distribution can be modeled as a probabilistic density $\mu(\theta|y)$. Compared with SDS that optimizes for the single θ, VPSD optimizes for the whole distribution μ, from which we can sample θ. Motivated by previous particle-based variational inference methods, we maintain k groups of vector parameters $\{\theta\}_{i=1}^k$ as particles to estimate the distribution μ, and $\theta(i)$ will be sampled from the optimal distribution μ^* if the optimization converges. This optimization can be realized through two score functions: one that approximates the optimal distribution with a noisy real image, and one that represents the current distribution with a noisy rendered image. The score function of noisy real images can be approximated by the pretrained diffusion model [26] $\epsilon_\phi(\mathbf{z}_t; y, t)$. The score function of noisy rendered images is estimated by another noise prediction network $\epsilon_{\phi_{\text{est}}}(\mathbf{z}_t; y, p, c, t)$, which is trained on the rendered images by $\{\theta\}_{i=1}^k$. The gradient of VPSD can be formed as,

$$\nabla_\theta \mathcal{L}_{\text{VPSD}}(\phi, \phi_{\text{est}}, \mathbf{x} = \mathcal{R}(\theta)) \triangleq \mathbb{E}_{t,\epsilon,p,c}\left[w(t)(\epsilon_\phi(\mathbf{z}_t; y, t) - \epsilon_{\phi_{\text{est}}}(\mathbf{z}_t; y, p, c, t)) \frac{\partial \mathbf{z}}{\partial \theta} \right] \tag{4}$$

where p and c in $\epsilon_{\phi_{\text{est}}}$ indicate control point variables and color variables, the weighting function $w(t)$ is a hyperparameter. And $t \sim \mathcal{U}(0.05, 0.95)$.

In practice, as suggested by [45], we parameterize ϵ_ϕ using a LoRA (Low-rank adaptation [10]) of the pretrained diffusion model. The rendered image not only serves to calculate the VPSD gradient but also gets updated by LoRA,

$$\mathcal{L}_{\text{lora}} = \mathbb{E}_{t,\epsilon,p,c} \left\| \epsilon_{\phi_{\text{est}}}(\mathbf{z}_t; y, p, c, t) - \epsilon \right\|_2^2 \tag{5}$$

where ϵ is the Gaussian noise. Only the parameters of the LoRA model will be updated, while the parameters of other diffusion models will remain unchanged to minimize computational complexity.

In [45], only randomly selected particles update the LoRA network in each iteration. However, this approach neglects the learning progression of vector particles, which are used to represent the optimal SVG distributions. Furthermore, these networks typically require numerous iterations to approximate the theoretical optimal distribution, resulting in slow convergence. In VPSD, we introduce a Reward Feedback Learning method, as Fig. 3 illustrates. This method leverages a pre-trained reward model [49] to assign reward scores to samples collected from LoRA model. Then LoRA model subsequently updates from these reweighted samples,

$$\mathcal{L}_{\text{reward}} = \lambda \mathbb{E}_y \left[\psi(r(y, g_{\phi_{\text{est}}}(y))) \right] \tag{6}$$

where $g_{\phi_{\text{est}}}(y)$ denotes the generated image of μ model with parameters ϕ_{est} corresponding to prompt y, and r represents the pretrained reward model [49], ψ represents reward-to-loss map function implemented by ReLU, and $\lambda = 1e-3$. We used the DDIM [32] to rapidly sample k samples during the early iteration stage. This method saves 2 times the iteration step for VPSD convergence and improves the aesthetic score of the SVG by filtering out samples with low reward values in LoRA.

Our final VPSD objective is then defined by the weighted average of the three terms,

$$\min_\theta \nabla_\theta \mathcal{L}_{\text{VPSD}} + \mathcal{L}_{\text{lora}} + \lambda_{\text{r}} \mathcal{L}_{\text{reward}} \tag{7}$$

where λ_{r} indicates reward feedback strength.

3.3. Vector Representation Primitives

In addition to text prompts, SVGDreamer provides a variety of vector representations for style control. These vector representations are achieved by limiting primitive types and their parameters. Users can control the art style generated by SVGDreamer by modifying the input text or by constraining the set of primitives and parameters. We explore six settings: 1) **Iconography** is the most common SVG style, consists of several paths and their fill colors.



Figure 4. **Qualitative comparison of different methods.** Note that DiffSketcher was originally designed for vector sketch generation; therefore, we re-implemented it to generate RGB vector graphics.

This style allows for a wide range of compositions while maintaining a minimalistic expression. We utilize closed form Bézier curves with trainable control points and fill colors. 2) **Sketch** is a way to convey information with minimal expression. We use open form Bézier curves with trainable control points and opacity. 3) **Pixel Art** is a popular videogame inspired style, frequently used for character and background art. We use square SVG polygons with fill colors. 4) **Low-Poly** is to consciously cut and pile up a certain number of simple geometric shapes according to the modeling laws of objects. We use square SVG polygons with trainable control points and fill colors. 5) **Painting** is a means of approximating the painter's painting style in vector graphics. We use open form Bézier curves with trainable control points, stroke colors and stroke widths. 6) **Ink and Wash Painting** is a traditional Chinese art form that utilizes varying concentrations of black ink. We use open form Bézier curves with trainable control points, opacity, and stroke widths.

4. Experiments

4.1. Qualitative Evaluation

Figure 4 presents a qualitative comparison between SVGDreamer and existing text-to-SVG methods. Compared to CLIPDraw [4], SVGDreamer synthesizes SVGs with higher fidelity and detail. We also compare our work with SDS-based methods [12, 48], emphasizing our ability to address issues such as shape over-smoothing and color oversaturation. As shown in the fifth column, SIVE achieves semantic decoupling but cannot overcome the inherently smooth nature of SDS. As observed in the last two columns, our approach demonstrates superior detail compared to the SDS-based approach, regardless of whether the model was optimized from scratch or through the entire process. Consequently, this leads to a higher aesthetic score.

4.2. Quantitative Evaluation

To demonstrate the effectiveness of our proposed method, we conducted comprehensive experiments to evaluate the model across various aspects, including Fréchet Inception Distance (FID) [6], Peak Signal-to-Noise Ratio (PSNR) [9], CLIPScore [23], BLIPScore [13], Aesthetic score [29] and Human Performance Score [47] (HPS). Table 1 presents a comparison of our approach with the most representative text-to-SVG methods, including CLIPDraw [4], VectorFusion [12], and DiffSketcher [48]. We conducted a quantitative evaluation of the six styles identified in Sec. 3.3, with each style comprising 10 unique prompts and 50 synthesized SVGs per prompt. For diversity evaluation of vector graphics and fill color saturation, we used SD sampling results as a Ground Truth (GT) and calculated FID and PSNR metrics respectively. The quantitative analysis in the first two columns indicates that our method surpasses other methods in terms of FID and PSNR. This suggests that our method offers a greater range of diversity compared to SDS-based synthesis [12, 48]. To assess the consistency between the generated SVGs and the provided text prompts, we used both CLIPScore and BLIPScore. To measure the perceptual quality of synthetic vector images, we measure aesthetic scores using the LAION aesthetic classifier [29]. Besides, we use HPS to evaluate our approach from a human aesthetic perspective.

4.3. Ablation Study

4.3.1 SIVE v.s. LIVE [17]

LIVE [17] offers a comprehensive image vectorization process that optimizes the vector graph in a hierarchical, layer-wise fashion. However, as Fig. 6 illustrates, LIVE struggles to accurately capture and distinguish between various subjects within an image, which can result in the same paths being superimposed on different visual subjects. When tasked with representing complex vector graphics requiring a greater number of paths, LIVE tends to superimpose path

Table 1. Quantitative evaluation of various Text-to-SVG methods.

Method / Metric	FID [6]↓	PSNR [9]↑	CLIPScore [23]↑	BLIPScore [13]↑	Aesthetic [29]↑	HPS [47]↑
CLIPDraw [4]	160.64	8.35	0.2486	0.3933	3.9803	0.2347
VectorFusion (scratch) [12]	119.55	6.33	0.2298	0.3803	4.5165	0.2334
VectorFusion [12]	100.68	8.01	0.2720	0.4291	4.9845	0.2450
DiffSketcher(RGB) [48]	118.70	6.75	0.2402	0.4185	4.1562	0.2423
SVGDreamer (from scratch)	84.04	10.48	0.2951	0.4311	5.1822	0.2484
+Reward Feedback	83.21	10.51	0.2988	0.4335	5.2825	0.2559
SVGDreamer	**59.13**	**14.54**	**0.3001**	**0.4623**	**5.5432**	**0.2685**

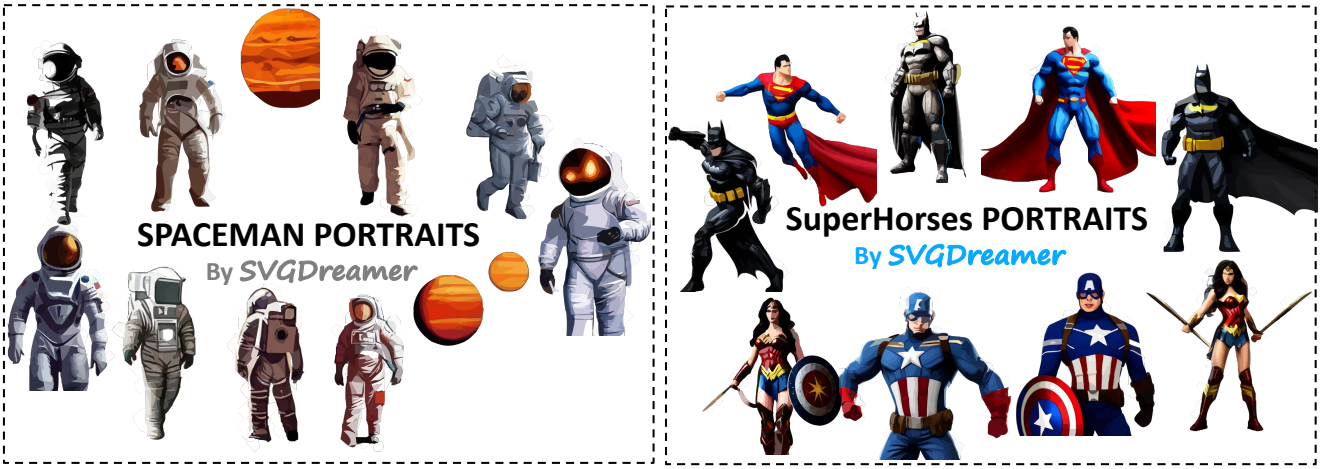


Figure 5. **Examples of vector assets created by SVGDreamer.** We specify foreground content as an SVG asset through a text prompt. To create assets that fit the SVG style, such as flat polygon vector, we constrain the vector representation via using a different prompt modifier to encourage the appropriate style: * ... on a white background, full body action pose, complete body, concept art, flat 2d vector icon.

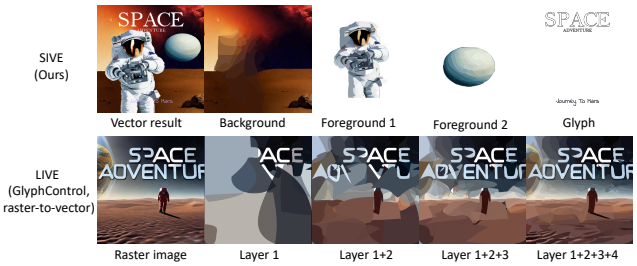


Figure 6. **Comparison of LIVE vectorization with SIVE.** In the first row, "Foreground 1" and "Foreground 2" refer to *Astronaut* and *Plants*, respectively. Glyphs have been added manually and were not produced by our method. In the LIVE setup, we follow the protocol outlined in VectorFusion [12], which represents a vector image with 128 paths distributed across four layers, with 32 paths in each layer.

hierarchies across different objects, complicating the SVG representation and making it difficult to edit. The resulting SVGs often contain complex and redundant shapes that can be inconvenient for further editing.

In contrast, SIVE is capable of generating succinct SVG forms with semantic-driven structures that align more closely with human perception. SIVE efficiently assigns paths to objects, enabling object-level vectorization.

4.3.2 VPSD v.s. LSDS [11, 12] v.s. ASDS [48]

The development of text-to-SVG [12, 48] was inspired by DreamFusion [22], but the resulting vector graphics have limited quality and exhibit a similar over-smoothness as the DreamFusion reconstructed 3D models. The main distinction between ASDS and LSDS lies in the augmentation of the input data. As demonstrated in Table 1 and Fig. 4, our approach demonstrates superior performance compared to the SDS-based approach in terms of FID. This indicates that our method is able to maintain a higher level of diversity without being affected by mode-seeking disruptions. Additionally, our approach achieves a higher PSNR compared to the SDS-based approach, suggesting that our method avoids the issue of supersaturation caused by averaging colors.

4.4. Applications of SVGDreamer

Our proposed tool, SVGDreamer, is capable of generating vector graphics with exceptional editability. Therefore, it can be utilized to create vector graphic assets for poster and

logo design. As shown in Fig. 5, all graphic elements in the two poster examples are generated by our SVGDreamer. Designers can easily recombine these elements with glyph to create unique posters. Additional examples of posters and logo designs can be found in Supplementary.

5. Conclusion

In this work, we have introduced SVGDreamer, an innovative model for text-guided vector graphics synthesis. SVGDreamer incorporates two crucial technical designs: Semantic-Driven Image Vectorization (SIVE) and Vectorized Particle-Based Score Distillation (VPSD). These empower our model to generate vector graphics with high editability, superior visual quality, and notable diversity. SVGDreamer is expected to significantly advance the application of text-to-SVG models in the design field.

Limitations. The editability of our method, which depends on the text-to-image (T2I) model used, is currently limited. However, future advancements in T2I diffusion models could enhance the decomposition capabilities of our approach, thereby extending its editability. Moreover, exploring ways to automatically determine the number of control points at the SIVE object level is valuable.

Acknowledgement. This work is supported by the CCF-Baidu Open Fund Project and Young Elite Scientists Sponsorship Program by CAST.

References

[1] Alexandre Carlier, Martin Danelljan, Alexandre Alahi, and Radu Timofte. Deepsvg: A hierarchical generative network for vector graphics animation. *Advances in Neural Information Processing Systems (NIPS)*, 33:16351–16361, 2020. 2

[2] Jingye Chen, Yupan Huang, Tengchao Lv, Lei Cui, Qifeng Chen, and Furu Wei. Textdiffuser: Diffusion models as text painters. *arXiv preprint arXiv:2305.10855*, 2023. 1

[3] Patrick Esser, Robin Rombach, and Bjorn Ommer. Taming transformers for high-resolution image synthesis. In *Proceedings of the IEEE/CVF conference on computer vision and pattern recognition (NIPS)*, pages 12873–12883, 2021. 5

[4] Kevin Frans, Lisa Soros, and Olaf Witkowski. CLIPDraw: Exploring text-to-drawing synthesis through language-image encoders. In *Advances in Neural Information Processing Systems (NIPS)*, 2022. 1, 2, 7, 8

[5] David Ha and Douglas Eck. A neural representation of sketch drawings. In *International Conference on Learning Representations (ICLR)*, 2018. 2

[6] Martin Heusel, Hubert Ramsauer, Thomas Unterthiner, Bernhard Nessler, and Sepp Hochreiter. Gans trained by a two time-scale update rule converge to a local nash equilibrium. *Advances in neural information processing systems (NIPS)*, 30, 2017. 7, 8

[7] Jonathan Ho and Tim Salimans. Classifier-free diffusion guidance. *arXiv preprint arXiv:2207.12598*, 2022. 2, 5

[8] Jonathan Ho, Ajay Jain, and Pieter Abbeel. Denoising diffusion probabilistic models. In *Advances in Neural Information Processing Systems (NIPS)*, pages 6840–6851, 2020. 2

[9] Alain Horé and Djemel Ziou. Image quality metrics: Psnr vs. ssim. In *2010 20th International Conference on Pattern Recognition*, pages 2366–2369, 2010. 7, 8

[10] Edward J Hu, yelong shen, Phillip Wallis, Zeyuan Allen-Zhu, Yuanzhi Li, Shean Wang, Lu Wang, and Weizhu Chen. LoRA: Low-rank adaptation of large language models. In *International Conference on Learning Representations (ICLR)*, 2022. 2, 6, 7, 8

[11] Shir Iluz, Yael Vinker, Amir Hertz, Daniel Berio, Daniel Cohen-Or, and Ariel Shamir. Word-as-image for semantic typography. *ACM Transactions on Graphics (TOG)*, 42(4), 2023. 2, 6, 8

[12] Ajay Jain, Amber Xie, and Pieter Abbeel. Vectorfusion: Text-to-svg by abstracting pixel-based diffusion models. In *Proceedings of the IEEE/CVF Conference on Computer Vision and Pattern Recognition (CVPR)*, 2023. 1, 2, 4, 5, 6, 7, 8

[13] Junnan Li, Dongxu Li, Caiming Xiong, and Steven Hoi. Blip: Bootstrapping language-image pre-training for unified vision-language understanding and generation. In *International Conference on Machine Learning (ICML)*, pages 12888–12900. PMLR, 2022. 7, 8

[14] Tzu-Mao Li, Michal Lukáč, Gharbi Michaël, and Jonathan Ragan-Kelley. Differentiable vector graphics rasterization for editing and learning. *ACM Transactions on Graphics (TOG)*, 39(6):193:1–193:15, 2020. 1, 2, 4

[15] Chen-Hsuan Lin, Jun Gao, Luming Tang, Towaki Takikawa, Xiaohui Zeng, Xun Huang, Karsten Kreis, Sanja Fidler, Ming-Yu Liu, and Tsung-Yi Lin. Magic3d: High-resolution text-to-3d content creation. In *Proceedings of the IEEE/CVF Conference on Computer Vision and Pattern Recognition (CVPR)*, pages 300–309, 2023. 4

[16] Raphael Gontijo Lopes, David Ha, Douglas Eck, and Jonathon Shlens. A learned representation for scalable vector graphics. In *Proceedings of the IEEE/CVF International Conference on Computer Vision (ICCV)*, 2019. 2

[17] Xu Ma, Yuqian Zhou, Xingqian Xu, Bin Sun, Valerii Filev, Nikita Orlov, Yun Fu, and Humphrey Shi. Towards layer-wise image vectorization. In *Proceedings of the IEEE/CVF Conference on Computer Vision and Pattern Recognition (CVPR)*, pages 16314–16323, 2022. 2, 4, 7

[18] Ben Mildenhall, Pratul P Srinivasan, Matthew Tancik, Jonathan T Barron, Ravi Ramamoorthi, and Ren Ng. Nerf: Representing scenes as neural radiance fields for view synthesis. *Communications of the ACM*, 65(1):99–106, 2021. 4

[19] Piotr Mirowski, Dylan Banarse, Mateusz Malinowski, Simon Osindero, and Chrisantha Fernando. Clip-clop: Clip-guided collage and photomontage. *arXiv preprint arXiv:2205.03146*, 2022. 1, 2

[20] Alexander Quinn Nichol, Prafulla Dhariwal, Aditya Ramesh, Pranav Shyam, Pamela Mishkin, Bob Mcgrew, Ilya Sutskever, and Mark Chen. GLIDE: Towards photorealistic image generation and editing with text-guided diffusion

models. In *Proceedings of the 39th International Conference on Machine Learning (ICML)*, pages 16784–16804, 2022. 1, 2

[21] Xingang Pan, Bo Dai, Ziwei Liu, Chen Change Loy, and Ping Luo. Do 2d {gan}s know 3d shape? unsupervised 3d shape reconstruction from 2d image {gan}s. In *International Conference on Learning Representations (ICLR)*, 2021. 4

[22] Ben Poole, Ajay Jain, Jonathan T. Barron, and Ben Mildenhall. Dreamfusion: Text-to-3d using 2d diffusion. In *The Eleventh International Conference on Learning Representations (ICLR)*, 2023. 2, 4, 5, 6, 8

[23] Alec Radford, Jong Wook Kim, Chris Hallacy, Aditya Ramesh, Gabriel Goh, Sandhini Agarwal, Girish Sastry, Amanda Askell, Pamela Mishkin, Jack Clark, et al. Learning transferable visual models from natural language supervision. In *International Conference on Machine Learning (ICML)*, pages 8748–8763. PMLR, 2021. 1, 2, 7, 8

[24] Aditya Ramesh, Prafulla Dhariwal, Alex Nichol, Casey Chu, and Mark Chen. Hierarchical text-conditional image generation with clip latents. *arXiv preprint arXiv:2204.06125*, 2022. 1, 2

[25] Pradyumna Reddy, Michael Gharbi, Michal Lukac, and Niloy J Mitra. Im2vec: Synthesizing vector graphics without vector supervision. In *Proceedings of the IEEE/CVF Conference on Computer Vision and Pattern Recognition (CVPR)*, pages 7342–7351, 2021. 2

[26] Robin Rombach, Andreas Blattmann, Dominik Lorenz, Patrick Esser, and Björn Ommer. High-resolution image synthesis with latent diffusion models. In *Proceedings of the IEEE/CVF Conference on Computer Vision and Pattern Recognition (CVPR)*, pages 10684–10695, 2022. 1, 2, 4, 6

[27] Chitwan Saharia, William Chan, Saurabh Saxena, Lala Li, Jay Whang, Emily L Denton, Kamyar Ghasemipour, Raphael Gontijo Lopes, Burcu Karagol Ayan, Tim Salimans, et al. Photorealistic text-to-image diffusion models with deep language understanding. In *Advances in Neural Information Processing Systems (NIPS)*, pages 36479–36494, 2022. 1, 2, 4

[28] Peter Schaldenbrand, Zhixuan Liu, and Jean Oh. Styleclipdraw: Coupling content and style in text-to-drawing synthesis. *arXiv preprint arXiv:2111.03133*, 2022. 1, 2

[29] Christoph Schuhmann. Improved aesthetic predictor. https://github.com/christophschuhmann/improved-aesthetic-predictor, 2022. 7, 8

[30] I-Chao Shen and Bing-Yu Chen. Clipgen: A deep generative model for clipart vectorization and synthesis. *IEEE Transactions on Visualization and Computer Graphics*, 28 (12):4211–4224, 2022. 2

[31] Jascha Sohl-Dickstein, Eric Weiss, Niru Maheswaranathan, and Surya Ganguli. Deep unsupervised learning using nonequilibrium thermodynamics. In *Proceedings of the International Conference on Machine Learning (ICML)*, pages 2256–2265, 2015. 2

[32] Jiaming Song, Chenlin Meng, and Stefano Ermon. Denoising diffusion implicit models. In *International Conference on Learning Representations (ICLR)*, 2021. 6

[33] Yang Song and Stefano Ermon. Generative modeling by estimating gradients of the data distribution. In *Advances in Neural Information Processing Systems (NIPS)*, 2019. 2

[34] Yiren Song and Yuxuan Zhang. Clipfont: Text guided vector wordart generation. In *33rd British Machine Vision Conference 2022, BMVC 2022, London, UK, November 21-24, 2022*, 2022. 1

[35] Yang Song, Jascha Sohl-Dickstein, Diederik P Kingma, Abhishek Kumar, Stefano Ermon, and Ben Poole. Score-based generative modeling through stochastic differential equations. In *International Conference on Learning Representations (ICLR)*, 2021. 2

[36] Yiren Song, Xuning Shao, Kang Chen, Weidong Zhang, Zhongliang Jing, and Minzhe Li. Clipvg: Text-guided image manipulation using differentiable vector graphics. In *Proceedings of the Conference on Artificial Intelligence (AAAI)*, 2023. 2

[37] StabilityAI. If by deepfloyd lab at stabilityai. https://github.com/deep-floyd/IF, 2023. 1, 2

[38] Hao Su, Xuefeng Liu, Jianwei Niu, Jiahe Cui, Ji Wan, Xinghao Wu, and Nana Wang. Marvel: Raster gray-level manga vectorization via primitive-wise deep reinforcement learning. *IEEE Transactions on Circuits and Systems for Video Technology (T-CSVT)*, 2023. 2

[39] Yingtao Tian and David Ha. Modern evolution strategies for creativity: Fitting concrete images and abstract concepts. In *Artificial Intelligence in Music, Sound, Art and Design*, pages 275–291. Springer, 2022. 2

[40] Yael Vinker, Ehsan Pajouheshgar, Jessica Y Bo, Roman Christian Bachmann, Amit Haim Bermano, Daniel Cohen-Or, Amir Zamir, and Ariel Shamir. Clipasso: Semantically-aware object sketching. *ACM Transactions on Graphics (TOG)*, 41(4):1–11, 2022. 1, 2

[41] Yael Vinker, Yuval Alaluf, Daniel Cohen-Or, and Ariel Shamir. Clipascene: Scene sketching with different types and levels of abstraction. In *Proceedings of the IEEE/CVF International Conference on Computer Vision (ICCV)*, pages 4146–4156, 2023. 1

[42] Haochen Wang, Xiaodan Du, Jiahao Li, Raymond A. Yeh, and Greg Shakhnarovich. Score jacobian chaining: Lifting pretrained 2d diffusion models for 3d generation. In *Proceedings of the IEEE/CVF Conference on Computer Vision and Pattern Recognition (CVPR)*, pages 12619–12629, 2023. 4

[43] Yizhi Wang and Zhouhui Lian. Deepvecfont: Synthesizing high-quality vector fonts via dual-modality learning. *ACM Transactions on Graphics (TOG)*, 40(6), 2021. 2

[44] Yizhi Wang, Gu Pu, Wenhan Luo, Pengfei Wang, Yexin ans Xiong, Hongwen Kang, Zhonghao Wang, and Zhouhui Lian. Aesthetic text logo synthesis via content-aware layout inferring. In *Proceedings of the IEEE/CVF Conference on Computer Vision and Pattern Recognition (CVPR)*, 2022. 2

[45] Zhengyi Wang, Cheng Lu, Yikai Wang, Fan Bao, Chongxuan Li, Hang Su, and Jun Zhu. Prolificdreamer: High-fidelity and diverse text-to-3d generation with variational score distillation. *arXiv preprint arXiv:2305.16213*, 2023. 4, 6

[46] Ronghuan Wu, Wanchao Su, Kede Ma, and Jing Liao. Iconshop: Text-based vector icon synthesis with autoregressive transformers. *arXiv preprint arXiv:2304.14400*, 2023. 2

[47] Xiaoshi Wu, Keqiang Sun, Feng Zhu, Rui Zhao, and Hongsheng Li. Human preference score: Better aligning text-to-image models with human preference. In *Proceedings of the IEEE/CVF International Conference on Computer Vision (ICCV)*, pages 2096–2105, 2023. 7, 8

[48] Ximing Xing, Chuang Wang, Haitao Zhou, Jing Zhang, Qian Yu, and Dong Xu. Diffsketcher: Text guided vector sketch synthesis through latent diffusion models. In *Advances in Neural Information Processing Systems (NIPS)*, 2023. 1, 2, 4, 5, 6, 7, 8

[49] Jiazheng Xu, Xiao Liu, Yuchen Wu, Yuxuan Tong, Qinkai Li, Ming Ding, Jie Tang, and Yuxiao Dong. Imagereward: Learning and evaluating human preferences for text-to-image generation, 2023. 2, 6, 4, 8

[50] Yukang Yang, Dongnan Gui, Yuhui Yuan, Haisong Ding, Han Hu, and Kai Chen. Glyphcontrol: Glyph conditional control for visual text generation. 2023. 1

SVGDreamer: Text Guided SVG Generation with Diffusion Model

Supplementary Material

Overview

This supplementary material is organized into several sections that provide additional details and analysis related to our work on SVGDreamer. Specifically, it will cover the following aspects:

- In section A, we present additional qualitative results of SVGDreamer, demonstrating its ability to generate SVGs with high editability, visual quality, and diversity.
- In section B, we demonstrate the potential applications of SVGDreamer in poster design and icon design.
- In section C, we provide more implementation details of SVGDreamer.
- In section D, We explain how to identify semantic objects in SIVE prompts.
- In section E, we conduct additional ablation studies to demonstrate the effects of CFG weights (see Appendix E.1), ReFL (see Appendix E.2), the number of vector particles (see Appendix E.3), and the number of paths (see Appendix E.4).
- In section F, we provide example results from using VPSD for raster image synthesis.
- In section G, we show the pseudo code of SVGDreamer. Code is available now [1].

A. Additional Qualitative Results

Editability. Our tool, SVGDreamer, is designed to generate high-quality vector graphics with versatile editable properties, empowering users to efficiently reuse synthesized vector elements and create new vector graphics. In our manuscript, Fig. 5 showcases two posters where each character is generated using SVGDreamer. Additionally, we present further examples in Fig. 7. These generated SVGs can be decomposed into background and foreground elements, which can then be recombined to create new SVGs.

Visual Quality and Diversity. In Fig. 8, we present additional examples generated by SVGDreamer, showcasing its ability to synthesize diverse object-level and scene-level vector graphics based on text prompts. Notably, our model can generate vector graphics with different styles, such as oil painting, watercolor, and sketch, by manipulating the type of primitives and text prompts. By incorporating the VPSD and ReFL into our model, SVGDreamer produces richer details compared to the state-of-the-art method VectorFusion.

It is important to highlight that our model can achieve different styles without relying on additional reference style images. Existing approaches for generating stylized vector graphics, such as StyleClipDraw, typically follow a style transfer pipeline used for raster images, which requires an additional style image as a reference. In contrast, SVGDreamer, being built upon a T2I model, can simply inject style information through text prompts. For instance, in the second example, we can obtain an oil painting in Van Gogh's style by using a text prompt.

B. Applications of SVGDreamer

In this section, we will demonstrate the utilization of SVGDreamer for synthesizing vector posters and icons.

Poster Design. A poster is a large sheet used for advertising events, films, or conveying messages to people. It usually contains text and graphic elements. While existing T2I models have been developing rapidly, they still face challenges in text generation and control. On the other hand, SVG offers greater ease in text control. In Fig. 9, we compare the posters generated by our SVGDreamer with those produced by four T2I models. It is important to note that all results generated by these T2I models are in raster format.

We will start by explaining the usage of our SVGDreamer tool for poster design. Initially, we employ SVGDreamer to generate graphic content. Then, we utilize modern font libraries to create vector fonts, taking advantage of SVG's transform properties to precisely control the font layout. Ultimately, we combine the vector images and fonts to produce comprehensive vector posters. To be more specific, we employ the FreeType font library [2] to represent glyphs using vectorized graphic outlines. In simpler terms, these glyph's outlines are composed of lines, Bézier curves, or B-Spline curves. This approach allows us to adjust and render the letters at any size, similar to other vector illustrations. The joint optimization of text and graphic content for enhanced visual quality is left for future work.

As depicted in Fig. 9, both Stable Diffusion [26] (the first column) and DeepFloyd IF [37] (the second column) display various text rendering errors, including missing glyphs, repeated or merged glyphs, and misshapen glyphs. GlyphControl [50] (the third column) occasionally omits individual letters, and the fonts obscure content, resulting in areas where the fonts appear to lack content objects. TextDiffuser [2] (the fifth column) is capable of generating fonts for different layouts, but it also suffers from the artifact of layout control masks, which disrupts the overall harmony of the content. In contrast, posters created using our SVGDreamer are not restricted by resolution size, ensuring the

[1] https://github.com/ximinng/SVGDreamer

[2] http://freetype.org/index.html

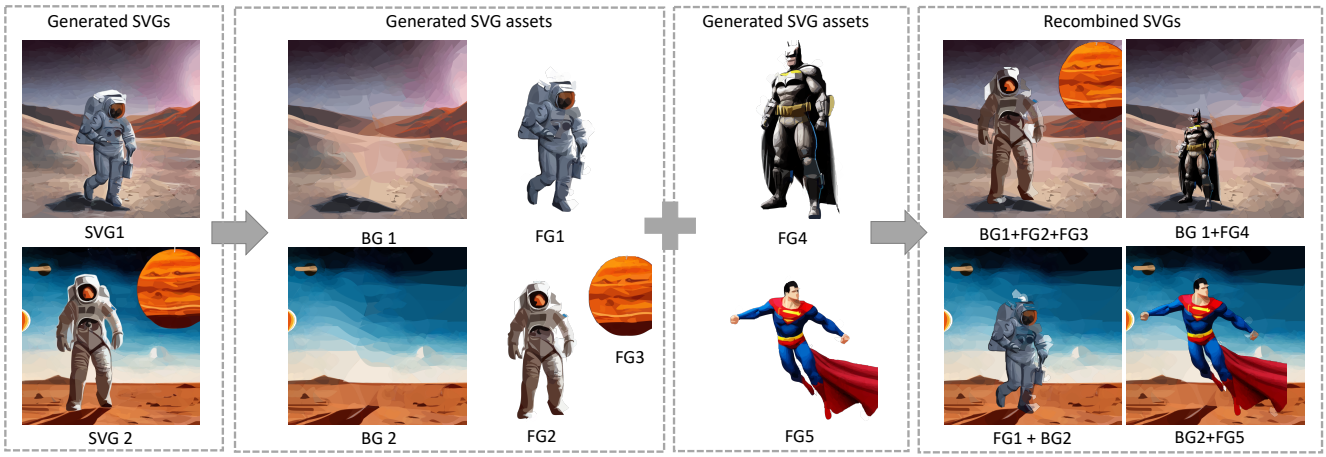


Figure 7. Examples showcasing the editability of the results generated by our SVGDreamer.

text remains clear and legible. Moreover, our approach offers the convenience of easily editing both fonts and layout, providing a more flexible poster design approach.

Icon Design. In addition to posters, SVGDreamer can be applied in icon design (as shown in the Fig. 10). We use SVGDreamer to obtain the graphic contents, and then create the polygon and circle layout by defining *def* tags in the SVG file. Then, we append the vector text paths to the end of the SVG file in order to obtain a complete vector icon.

C. Implementation Details

Our method is based on the pre-trained Stable Diffusion model [26]. We use the Adam optimizer with $\beta_1 = 0.9$, $\beta_2 = 0.9$, $\epsilon = 1e-6$ for optimizing SVG path parameters $\theta = \{P_i, C_i\}_{i=1}^{n}$. We use a learning rate warm-up strategy. In the first 50 iterations, we gradually increase the control point learning rate from 0.01 to 0.9, and then employ exponential decay from 0.8 to 0.4 in the remaining 650 iterations (a total of 700 iterations). For the color learning rate, we set it to 0.1 and the stroke width learning rate to 0.01. We adopt AdamW optimizer with $\beta_1 = 0.9$, $\beta_2 = 0.999$, $\epsilon = 1e-10$, $lr = 1e-5$ for the training of LoRA [10] parameters. In the majority of our experiments, we set the particle number k to 6, which means that 6 particles participate in the VPSD (Sec. 3.2), LoRA update, and ReFL update simultaneously. To ensure diversity and fidelity to text prompts in the synthesized SVGs, while maintaining rich details, we set the guidance scale of the Classifier-free Guidance (CFG [7]) to 7.5. During the optimization process, SVGDreamer requires at least 31 GB memory on an Nvidia-V100 GPU to produce 6 SVGs.

Synthesizing flat iconographic vectors, we allow path control points and fill colors to be optimized. During the course of optimization, many paths learn low opacity or shrink to a small area and are unused. To encourage usage of paths and therefore more diverse and detailed images, motivated by VectorFusion [12], we periodically reinitialize paths with fill-color opacity or area below a threshold. Reinitialized paths are removed from optimization and the SVG, and recreated as a randomly located and colored circle on top of existing paths.

D. Object Identification in SIVE Prompts

It is common for multiple nouns within a sentence to refer to the same object. We present two examples in Fig. 11. In our experiments, we did not employ a specific selection strategy because the cross-attention maps for such nouns-for example, "man" and "astronaut" – are very similar. Therefore, choosing either "man" or "astronaut" produces similar results with our method. For more precise control, users may utilize the cross-attention maps of the text prompt to identify the desired objects. In SIVE, users can use visual text prompts to identify semantic objects.

E. Additional Ablation Studies

Next, we provide additional ablation experiments to demonstrate the effectiveness of the proposed components.

E.1. Ablation on CFG [7] Weights

In this section, we explore how Classifier-free Guidances (CFG) [7] affects the diversity of generated results. For VPSD, we set the number of particles as 6 and run experiments with different CFG values. For LSDS [12], we run 4 times of generation with different random seeds. The results are shown in Fig. 12. As shown in the figure, smaller CFG provides more diversity. We conjecture that this is because the distribution of smaller guidance weights has more diverse modes. However, when the CFG becomes too small (e.g., CFG= 2), it cannot provide enough guidance to generate reasonable results. Therefore, in our implementation, we set CFG to 7.5 as a trade-off between diversity and op-

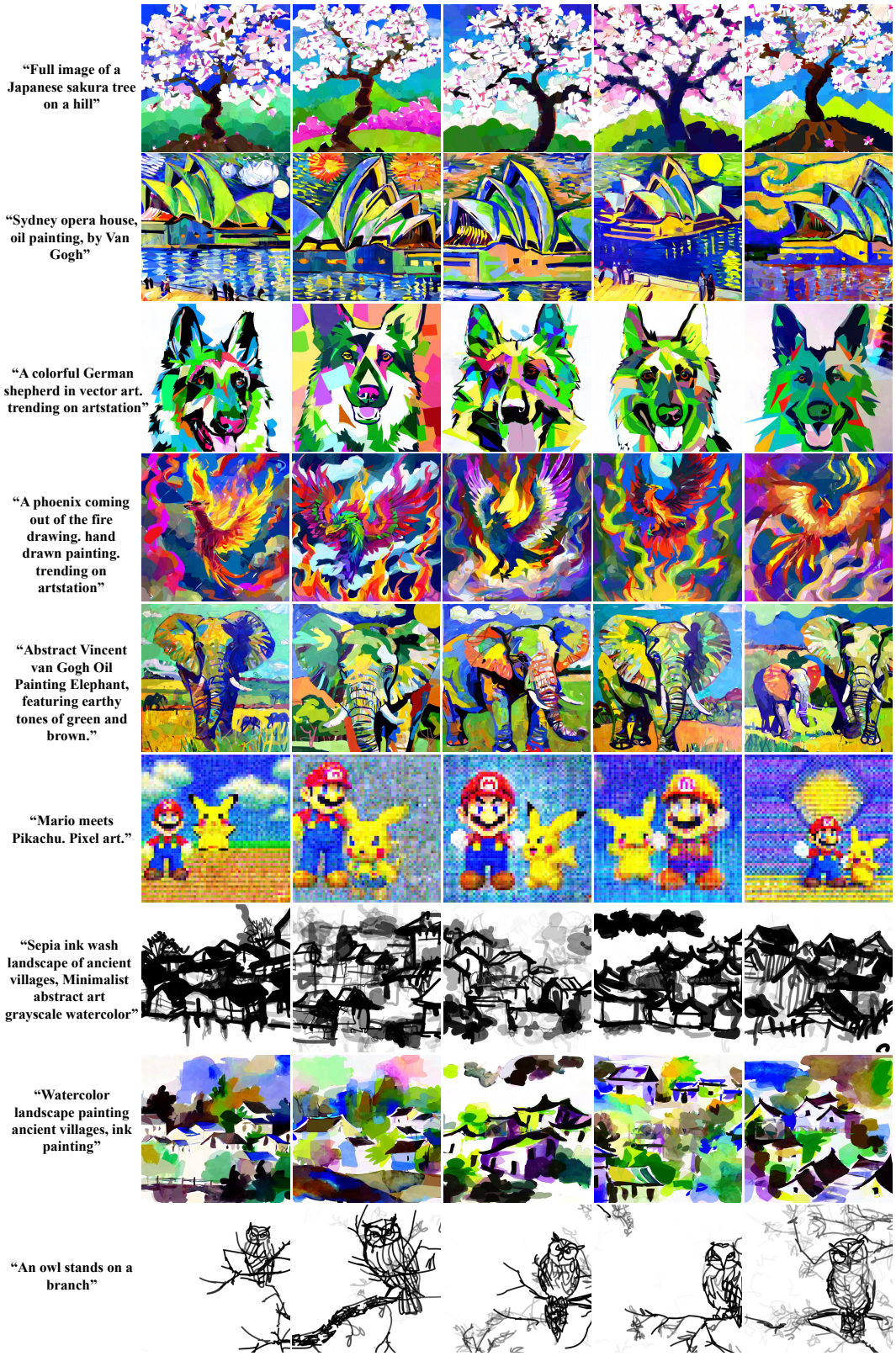


Figure 8. **More results generated by our SVGDreamer.** The style is governed by vector primitives.

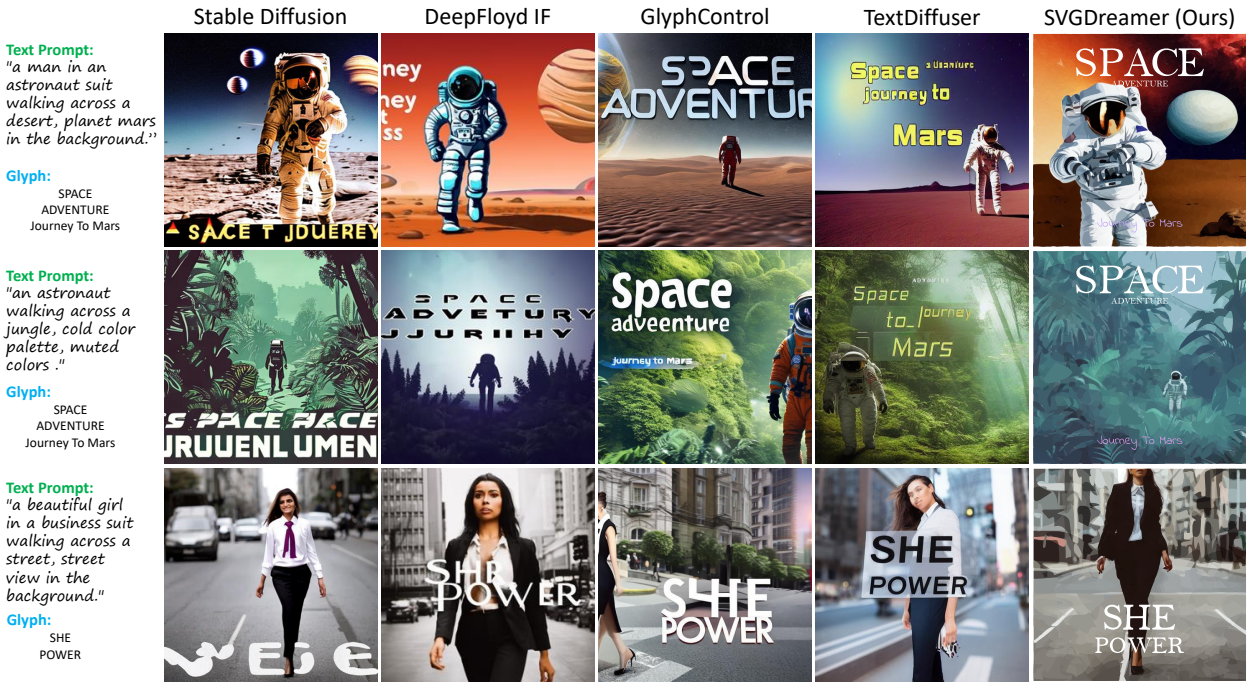


Figure 9. **Comparison of synthetic posters generated by different methods.** The input text prompts and glyphs to be added to the posters are displayed on the left side.



Figure 10. **Examples of synthetic icons.** Note that the glyphs are manually added.

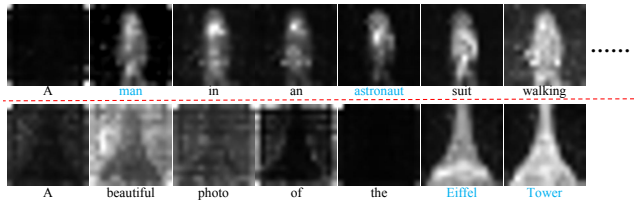


Figure 11. **Visualizations of the LDM cross-attention maps.**

timization stability. Note that SDS-based methods [12, 48] do not work well in such small CFG weights. Instead, our VPSD provides a trade-off option between CFG weight and diversity, and it can generate more diverse results by simply setting a smaller CFG.

E.2. Ablation on ReFL

In [45], only selected particles update the LoRA network in each iteration. However, this approach neglects the learning progression of LoRA networks, which are used to represent variational distributions. These networks typically require numerous iterations to approximate the optimal distribution, resulting in slow convergence. Unfortunately, the randomness introduced by particle initialization can lead to early learning of sub-optimal particles, which adversely affects the final convergence result. In VPSD, we introduce a Reward Feedback Learning (ReFL) method. This method leverages a pre-trained reward model [49] to assign reward scores to samples collected from LoRA model. Then LoRA model subsequently updates from these reweighted samples. As indicated in Table 2, this led to a significant reduction in the number of iterations by almost 50%, resulting in a 50% decrease in optimization time. And improves the aesthetic score of the SVG by filtering out samples with low reward values in LoRA. Filtering out samples with low reward values, as demonstrated in Table 1, enhances the aesthetic score of the SVG. The visual improvements brought by ReFL are illustrated in Fig. 13.

E.3. Ablation on the Number of Vector Particles

We investigate the impact of the number of particles on the generated results. We vary the number of particles in 1, 4, 8,

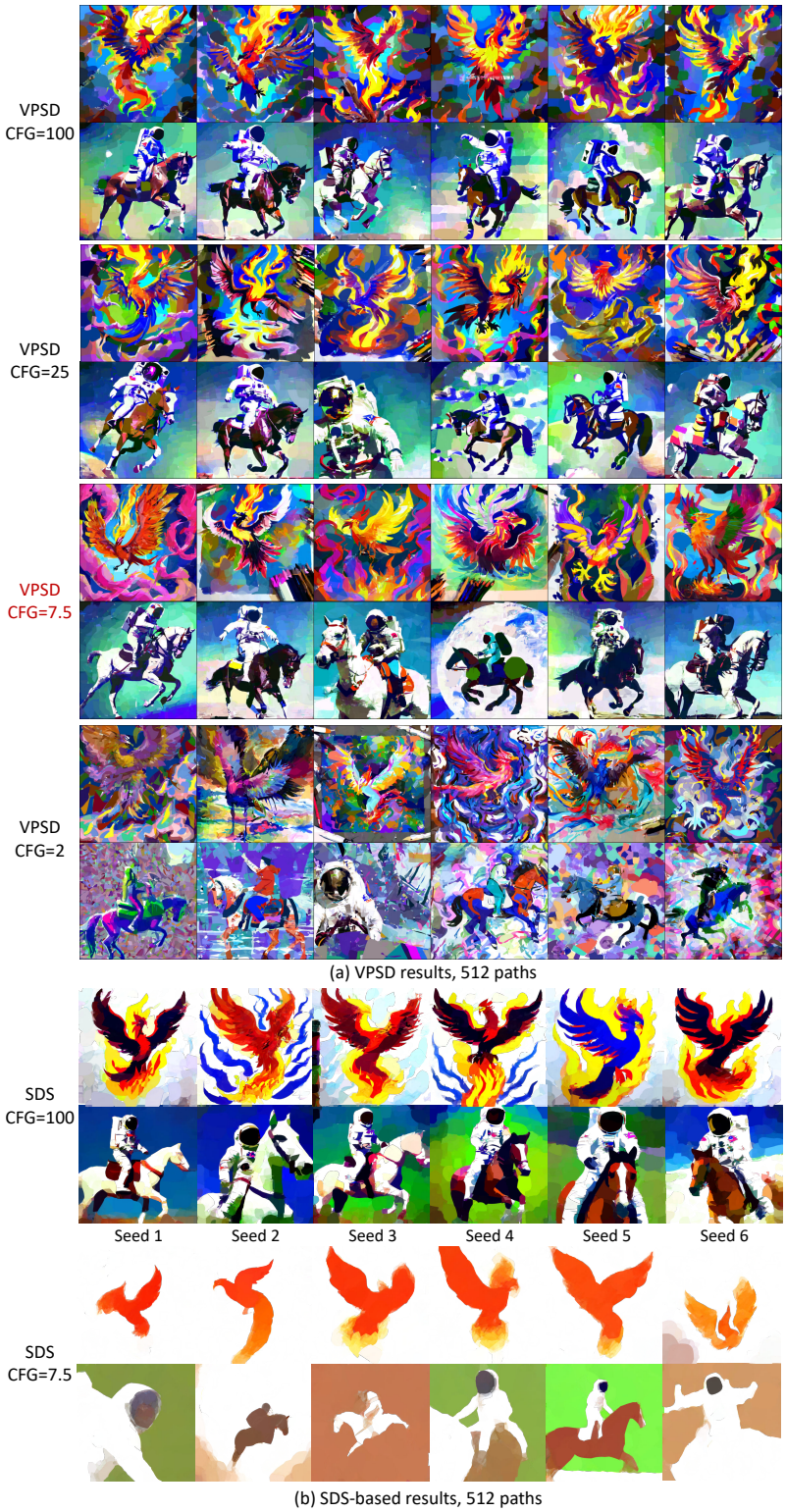


Figure 12. **Ablation on how Classifier-free Guidances (CFG) [7] weight affects the randomness.** Smaller CFG provides more diversity. But too small CFG provides less optimization stability. The prompt is "A photograph of an astronaut riding a horse".

16 and analyze how this variation affects the outcomes. The CFG of VPSD is set as 7.5. As shown in Fig. 14, the diversity of the generated results is slightly larger as the number of particles increases. Meanwhile, the quality of gen-



Figure 13. **Effect of the Reward Feedback Learning (ReFL)**. When employing ReFL, the visual quality of the generated results is significantly enhanced.



Figure 14. **Ablation on the number of particles.** The diversity of the generated results is slightly larger as the number of particles increases. The quality of generated results is not significantly affected by the number of particles. The prompt is "A photograph of an astronaut riding a horse".

erated results is not significantly affected by the number of particles. Considering the high computation overhead associated with optimizing vector primitive representations and the limitations imposed by available computation resources, we limit our testing to a maximum of 6 particles.

E.4. Ablation on the Number of Paths

This subsection analyzes the effect of different stroke numbers on VPSD synthetic vector images. Figure 15 shows examples with 128, 256, 512, and 768 paths, from top to bottom, using Iconography primitives. As the path count increases, the image transitions from abstract to more concrete, and the level of detail notably improves. VPSD offers superior visual details compared to SDS, including aspects

Table 2. Efficiency of our proposed ReFL in SVGDreamer.

Method	Canvas Size	Path Number	Iteration Steps	Time(min:sec)
W/O ReFL	224 * 224	128	500	13m15s
W ReFL	224 * 224	128	300	6m45s
W/O ReFL	600 * 600	256	500	14m21s
W ReFL	600 * 600	256	300	7m21s

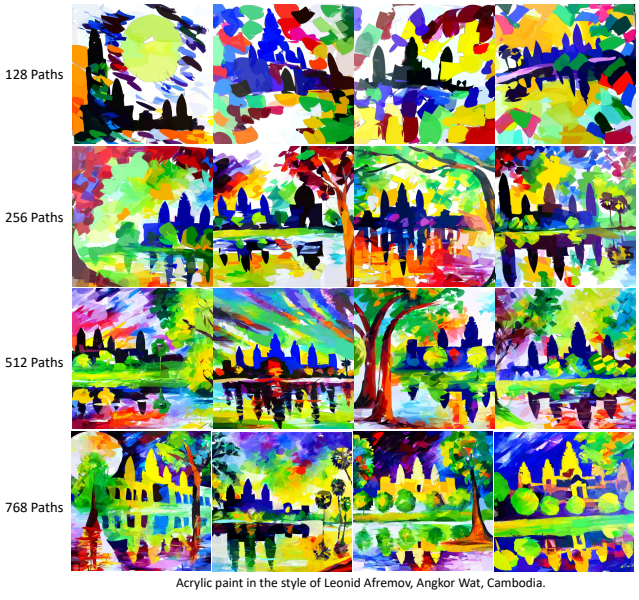


Figure 15. **Effect of the number of paths.** Adding vector paths can be synthesized to enhance SVG detail.



Figure 16. **2D image synthesis.** Comparison of the results from using VPSD and VSD for 2D image synthesis.

like water reflections. Additionally, VPSD better aligns with text prompts.

F. VPSD for 2D Image Synthesis

In this work, VPSD is specifically designed for text-to-SVG generation; however, it can also be adapted for 2D image synthesis. As illustrated in Fig. 16, images synthesized by VSD may exhibit displaced or incomplete object layouts, resulting in samples that might not meet human aesthetic preferences. In contrast, VPSD integrates a reward score within its feedback learning process, which significantly enhances the quality of the generated images.

G. Algorithm for VPSD

We summarize the algorithm of Vectorized Particle-based Score Distillation (VPSD) in Algorithm 1. First, VPSD initializes $k(\geq 1)$ groups of SVG parameters, a pretrained diffusion model ϵ_ϕ parameterized by ϕ and the LoRA layers $\epsilon_{\phi_{\text{est}}}$ parameterized by ϕ_{est}, as the pretrained reward model r. Note that only the diffusion model is pretrained with frozen parameters, while LoRA [10] thaws some of its parameters. Subsequently, VPSD randomly selects a parameter θ from the set of SVG parameters and generates a raster image x based on this selection. The parameter θ is then updated using Variational Score Distillation (VSD). k samples are sampled using $\epsilon_\phi(y)$ and utilized to update the parameters of ϕ. This process is repeated until a satisfactory result is obtained and the algorithm returns k groups of SVG parameters as the final output.

Algorithm 2 is the combination of VPSD and SIVE (Semantic-driven Image Vectorizatio). This algorithm has the same initialization as VPSD, but it needs to get a sample using diffusion model ϵ_ϕ given text prompt y. In the sampling process, it can obtain the sample's corresponding attention map. Depending on attention map, the algorithm can get background mask and foreground mask. It optimizes the SVG parameters according to the foreground mask and background mask, respectively, and then finetunes them using the VPSD algorithm.

Algorithm 1 Vectorized Particle-based Score Distillation (VPSD)

Require: Text prompt y. Number of particles k (≥ 1). Number of SVG primitives n (≥ 1). Pretrained Text-to-Img Diffusion Model ϵ_ϕ. Learning rates η_p for SVG path parameters. Learning rate η_e for diffusion model parameters. r represents the pretrained reward model [49]. λ_r indicates reward feedback strength.

Initialize: k groups of SVG parameters $\{\theta^{(1)}, \cdots, \theta^{(n)}\} = \{(P_j^{(i)}, C_j^{(i)})\}_{j=1}^n$, a pretrained diffusion model ϵ_ϕ is parameterized by ϕ, a LoRA [10] model $\epsilon_{\phi_{\text{est}}}$ is parameterized by ϕ_{est}, the pretrained reward model r.
while not converged **do**
  Randomly sample $\theta \sim \{\theta^{(i)}\}_{i=1}^k$.
  Render the SVG parameter θ to get a raster image $x = \mathcal{R}(\theta)$.
  $\theta \leftarrow \theta - \eta_p \mathbb{E}_{t,\epsilon,p,c}\left[\omega(t)(\epsilon_\phi(\mathbf{z}_t; y, t) - \epsilon_{\phi_{\text{est}}}(\mathbf{z}_t); y, p, c, t)\frac{\partial \mathbf{z}}{\partial \theta}\right]$
  Sample $w(\leq k)$ samples using $\epsilon_{\phi_{\text{est}}}(y)$.
  $\phi \leftarrow \phi - \eta_e \nabla_\phi \left[\mathbb{E}_{\epsilon,t}\left\|\epsilon_{\phi_{\text{est}}}(\mathbf{z}_t; y, p, c, t) - \epsilon\right\|_2^2 + \lambda_r \mathbb{E}_{y,w}\left[\psi(r(y, g_{\phi_{\text{est}}}(y)))\right]\right]$
end while
return $\{\theta_1, \cdots \theta_k\}$.

Algorithm 2 Semantic-driven Image Vectorization (SIVE) + VPSD

Require: Text prompt y. Number of particles k (≥ 1). Number of SVG primitives n (≥ 1). Pretrained Text-to-Img Diffusion Model ϵ_ϕ. Learning rates η_p for SVG path parameters. Learning rate η_e for diffusion model parameters. r represents the pretrained reward model [49]. λ_r indicates reward feedback strength.

Initialize: k groups of SVG parameters $\{\theta^{(1)}, \cdots, \theta^{(n)}\} = \{(P_j^{(i)}, C_j^{(i)})\}_{j=1}^n$, a noise prediction model ϵ_ϕ parameterized by ϕ.
Sample a sample using $\epsilon_\phi(y)$.
Get the attention map corresponding to the i-th text token $\mathcal{M}_{\text{FG}}^i = \text{softmax}(QK_i^T)/\sqrt{d}$
Get the background attention map $\mathcal{M}_{\text{BG}} = 1 - (\sum_{i=1}^O \mathcal{M}_{\text{FG}}^i)$
Get the background mask and foreground masks $\hat{\mathcal{M}} = \{\{\hat{\mathcal{M}}_{\text{FG}}\}_{o=1}^O, \hat{\mathcal{M}}_{\text{BG}}\}$, respectively.
while not converged **do**
  $\theta^{(1)} \leftarrow \theta^{(1)} - \eta_p \nabla_\theta \mathbb{E}_o(\hat{\mathcal{M}}_i \odot I - \hat{\mathcal{M}}_i \odot \mathbf{x})^2$
end while
Initialize: a LoRA [10] model $\epsilon_{\phi_{\text{est}}}$ is parameterized by ϕ_{est}, the pretrained reward model r.
while not converged **do**
  Randomly sample $\theta \sim \{\theta\}_{i=1}^k$.
  Render the SVG parameter θ to get a raster image $x = \mathcal{R}(\theta)$.
  $\theta \leftarrow \theta - \eta_p \mathbb{E}_{t,\epsilon,p,c}\left[\omega(t)(\epsilon_\phi(\mathbf{z}_t; y, t) - \epsilon_{\phi_{\text{est}}}(\mathbf{z}_t); y, p, c, t)\frac{\partial \mathbf{z}}{\partial \theta}\right]$
  Sample $w(\leq k)$ samples using $\epsilon_{\phi_{\text{est}}}(y)$.
  $\phi \leftarrow \phi - \eta_e \nabla_\phi \left[\mathbb{E}_{\epsilon,t}\left\|\epsilon_{\phi_{\text{est}}}(\mathbf{z}_t; y, p, c, t) - \epsilon\right\|_2^2 + \lambda_r \mathbb{E}_{y,w}\left[\psi(r(y, g_{\phi_{\text{est}}}(y)))\right]\right]$
end while
return $\{\theta_1, \cdots \theta_k\}$.